

Instabilities and transition in boundary layers

N VINOD and RAMA GOVINDARAJAN

Engineering Mechanics Unit, Jawaharlal Nehru Centre for Advanced Scientific Research,
Bangalore 560 064, India
E-mail: rama@jncasr.ac.in

Abstract. Some recent developments in boundary layer instabilities and transition are reviewed. Background disturbance levels determine the instability mechanism that ultimately leads to turbulence. At low noise levels, the traditional Tollmien–Schlichting route is followed, while at high levels, a ‘by-pass’ route is more likely. Our recent work shows that spot birth is related to the pattern of secondary instability in either route.

Keywords. Boundary layer; stability.

PACS Nos 47.27.Cn; 47.27.Nz

1. Background

The laminar–turbulent transition has been a subject of great interest for over a century, and will perhaps remain for sometime as one of the last frontiers in our understanding of turbulence. The mechanism of transition differs vastly from flow to flow and much needs to be done before a general theory emerges. The books by Lin [1], Chandrasekhar [2], Drazin and Reid [3], Huerre and Rossi [4] and Schmid and Henningson [5] offer detailed information on what is known. In open flows, such as jets, wakes and shear layers, the transition to turbulence is a process that usually occurs in a sequence of instability events. Most research in open flows has focussed on the boundary layer formed by the flow of fluid past a solid object. This is because research in this area was traditionally driven by the aircraft industry. A lot of knowledge has been gained about this flow but there still remain important gaps in our understanding. The present paper addresses one such gap, namely, the ‘end-game’ in the transition process, where flow changes character from laminar to transitional, i.e., with islands of turbulence in a laminar sea.

We begin by introducing the stages in the transition process, and many of the features described here are common to all shear flows. We then try to establish a connection between laminar instability and the birth of turbulent spots.

A schematic picture of the sequence of events is given in figure 1. An important characteristic of open flows is that the Reynolds number varies with the downstream distance x . This means that all the stages of the laminar–turbulent transition exist at different stream-wise location in one flow. At the leading edge (x close to zero)

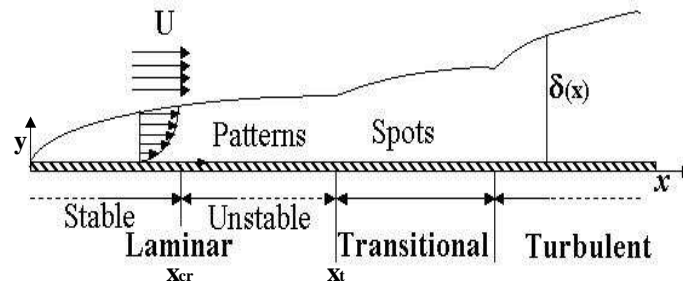


Figure 1. Sequence of events in the laminar–turbulent transition process on a boundary layer formed by the flow past a semi-infinite flat plate. The Reynolds number $R \equiv \delta U/\nu$ is an increasing function of the downstream distance.

the flow is laminar and far downstream (large x) the flow asymptotically goes to fully developed turbulence. We define the Reynolds number as $R \equiv UL/\nu$, where U is the local free stream velocity, ν is the kinematic viscosity and L is a length scale related to the boundary layer thickness. The transition process begins at low x with a *receptivity* stage, during which disturbances existing in the far-field or created by surface roughness, tunnel noise etc. are entrained into the laminar boundary layer and can create forced perturbations within. This stage is important, since the mechanism and the Reynolds number of transition can vary dramatically with both the amplitude and the spectral content of the external noise and the manner in which it is received within. The receptivity process is not well understood; here we do not discuss this. For the present discussion, we take the flow within the stable laminar boundary layer to contain small disturbances of all frequencies.

Above a critical Reynolds number R_{cr} , i.e., downstream of a certain stream-wise location x_{cr} , components of disturbances lying within a narrow range of frequencies begin to grow. This growth can be described by linear hydrodynamic stability theory and has been extensively studied for two-dimensional flows. In their pioneering work, Orr [6] and Sommerfeld [7] derived the famous Orr–Sommerfeld (OS) equation for the stability of viscous parallel laminar flows. The Orr–Sommerfeld equation is satisfied by the normal modes of the linear perturbation, and may be derived from the (here 2D) Navier–Stokes equation in a straightforward manner. Flow quantities are split into their mean and a linear perturbation in normal mode form. For example, the wall normal component v is expressed as

$$\hat{v}(x, y, t) = v(y) \exp[ik_p(x - ct)], \quad (1)$$

where y is the coordinate normal to the wall, t is the time, k_p is the stream-wise wave number and c is the complex wave speed. Eliminating the pressure term, using continuity and linearising the resulting equation, we get

$$(U - c)(v'' - k_p^2 v) - U''v = \frac{1}{ik_p R}(v^{iv} - 2k_p^2 v'' + k_p^4 v), \quad (2)$$

where U is the mean velocity, and the primes denote derivative with respect to y . The boundary conditions are $v = v' = 0$ at the wall and at $y \rightarrow \infty$. This equation

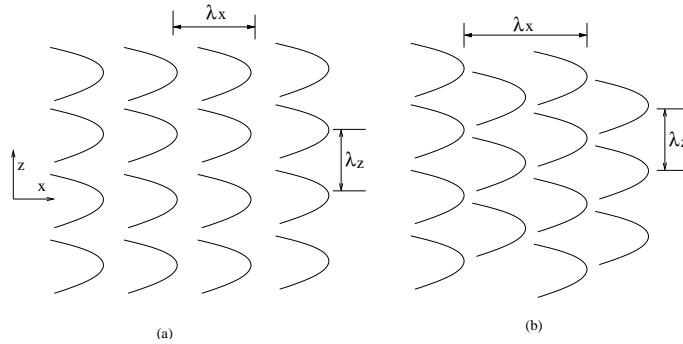


Figure 2. Schematic diagram of two types of breakdown. **(a)** *K*-type, where the stream-wise wavelength of the pattern is equal to that of the two-dimensional Tollmien–Schlichting waves ($\lambda_x = \lambda_{TS}$). **(b)** *N*-type/*H*-type, $\lambda_x = 2\lambda_{TS}$. The latter is most often the pattern observed.

was first solved by Tollmien [8] and Schlichting [9], and the growing disturbance waves predicted by them are now known as TS waves. In spite of these theoretical predictions, the existence of wave-like growing disturbances in laminar flow was a matter for debate until the landmark experiments of Schubaurer and Skramstad [10], who measured TS waves downstream of a vibrating ribbon, growing as they convect downstream. The first instabilities are two-dimensional [11]. At a sufficiently large x , the TS waves have grown to a significant amplitude. We now have an ‘almost-periodic’ flow, since the flow contains finite oscillations which are very slowly growing as they convect downstream. The new flow is now unstable to three-dimensional secondary modes [12], giving rise to Λ -shaped vortices (see e.g. [13–15]). The Λ vortices form a three-dimensional pattern, where the vortices could be aligned (*K*-type, figure 2a, [16,17]) or staggered (*N*-type/*H*-type, figure 2b, [17,18]).

The equations for secondary instability are formulated as before [12,19], with the difference that the basic flow is periodic (consisting of the laminar flow plus the most dominant oscillatory mode, denoted here by the subscript ‘p’ for ‘primary disturbance’):

$$\vec{U}(x, y, z, t) = \{ \bar{U}(y)\vec{i} + A_p[u_p(y)\vec{i} + v_p(y)\vec{j}] \times \exp[i(k_p x - \omega_p t)] \} + \vec{u}_s(x, y, z, t), \quad (3)$$

the quantity within the curly brackets is the periodic basic flow. Here A , k and ω stand for the amplitude, wave number and frequency of the disturbance respectively. The secondary disturbances appear in pairs, e.g.

$$u_s = \frac{1}{2} [u_+(y) \exp\{i(k_+ x + \beta z - \omega_+ t)\} + u_-(y) \exp\{i(k_- x - \beta z - \omega_- t)\} + \text{c.c.}] \quad (4)$$

The above ansatz is substituted into the Navier–Stokes and continuity equations, linear terms in the secondary are retained, and disturbance pressure and the stream-

wise component of the velocity are eliminated. On averaging over x , z and t , only the resonant modes survive, which are related as follows:

$$k_+ + k_- = k_p, \quad \text{and} \quad (\omega_+ + \omega_-)_r = \omega_p. \quad (5)$$

The final equations are

$$\begin{aligned} & \left[i(\omega_+ - k_+U) + \frac{1}{R}(D^2 - k_+^2 - \beta^2) \right] [(k_+^2 + \beta^2) f_+ - Dv_+] \\ & - ik_+U'v_+ - A_p \left(\frac{k_+}{2k_-} \right) \{ [ik_+u_pD + v_pD^2 + ik_-Du_p]v_-^* \\ & + [(\beta^2 - k_-k_+)v_pD + ik_+(k_-^2 + \beta^2)u_p]f_-^* \} = 0 \end{aligned} \quad (6)$$

and

$$\begin{aligned} & \left[i(\omega_+ - k_+U) + \frac{1}{R}(D^2 - k_+^2 - \beta^2) \right] (Df_+ - v_+) \\ & - ik_+U'f_+ + A_p \left(\frac{k_p + k_-}{2} \right) \left[\frac{v_p}{k_-}Dv_-^* - iu_p(v_-^* + Df_-^*) \right] \\ & + \frac{A_p}{2} \left[v_p \left(\frac{k_p\beta^2}{k_-} + D^2 \right) - ik_-(Du_p) \right] f_-^* = 0. \end{aligned} \quad (7)$$

The quantity f_+ ($\equiv -iw_{s+}/\beta$) is proportional to the span-wise component of the secondary disturbance velocity, and the operator D stands for differentiation with respect to y . The boundary conditions are

$$\mathbf{u}_s = 0 \quad \text{at } y = 0 \quad \text{and} \quad \mathbf{u}_s \rightarrow 0 \quad \text{as } y \rightarrow \infty. \quad (8)$$

Equations (6) and (7), along with two corresponding equations in v_-^* and f_-^* describe an eigenvalue problem for the secondary instability. The resulting flow contains a pattern of high- and low-disturbance vorticity as shown in figure 2.

Further downstream, i.e., in the short region downstream of the patterns and immediately upstream of x_t in figure 1, there follows a succession of events which are not completely understood even in a two-dimensional boundary layer. The location x_t is defined here as the onset of transition. The behaviour downstream of x_t is discussed in §3. Briefly, the flow now changes character: we see patches of turbulence (called turbulent spots). The spots grow both in the stream-wise and span-wise directions as they convect downstream with the flow [20]; in this process they often merge with neighbouring spots, until the flow asymptotically becomes fully turbulent (at some large x). The region surrounding the turbulent spots is laminar, but not quite of the same character as the flow upstream of x_t .

2. Transient growth of disturbances

The events upstream of x_t do not always occur as described above. When external disturbance levels are high, a laminar boundary layer can display high levels

of transient growth of disturbances even while being asymptotically stable, and ‘by-pass’ the linear and secondary growth stages [5]. Bypass transition can take place due to a variety of alternate mechanisms, such as the temporary algebraic growth of disturbances, or the breakdown due to a pair of growing oblique waves. We will discuss only the former in this paper. Another interesting but infrequent variant, which will not be discussed here, is the gradual filling up of the disturbance spectrum to obtain fully developed turbulence [18].

Let us now see how transient growth is created by a linear mechanism. An instance of algebraic growth of disturbances was provided by [21] for an inviscid flow. It was in the famous work of [22], where the mechanism for algebraic growth which could lead to transition to turbulence was explained. A shear flow contains a host of disturbance eigenmodes which satisfy the OS equation or variants of it. Each mode is exponentially decaying, but since the OS operator is not self-adjoint, the eigenfunctions are not orthogonal. The waves can thus interfere so that at short times the total disturbance kinetic energy grows algebraically. At long times, all the disturbances, if still behaving linearly, would of course decay exponentially, but if the temporary growth of disturbance kinetic energy is high enough, nonlinear mechanisms can take over at finite time, and drive the flow to turbulence. The likelihood of such *transient growth* in boundary layers has been evaluated (e.g., [23–26]). These studies show that in high disturbance environments, algebraic growth can be of sufficient magnitude to activate a transition to turbulence. It is seen that vorticity perturbations which are aligned in the stream-wise direction, and with a span-wise wavelength of the order of the boundary layer thickness [27] have the highest potential for transient energy amplification. Incidentally, the importance of stream-wise vortices, in producing turbulence was known to the community earlier, since Landahl [28,29] first introduced the *lift-up mechanism*. The stream-wise vortices serve to move low momentum fluid away from the wall, and high momentum fluid towards the wall, giving rise to ‘stream-wise streaks’, which are narrow elongated regions of lower or higher stream-wise speed than the surrounding fluid. Their characteristic shape is visualised by Boiko *et al* [30]. As time passes, the streaky pattern attains its maximum amplitude, and undergoes a secondary instability which deforms the pattern in the manner shown in figure 3 (from [5]) and causes breakdown to turbulence. From a linear inviscid stability analysis of the streaky boundary layer [23] it is seen that secondary instability is triggered when the disturbance amplitude exceeds 26% of the free-stream velocity.

More recently, experiments to check the occurrence of algebraic growth are being conducted for a variety of flows. The experiments of White [31] on a flat plate boundary layer show qualitative agreement with the theory. A streak was generated at the leading edge here and its downstream behaviour was observed. There were, however, quantitative discrepancies. For example, in the experiment, the maximum transient growth occurred well upstream of the location predicted by the theory. The wall-normal location of the maximum disturbance was different as well. Boiko and Chun [32] again study the evolution of a streak in a flat plate boundary layer, this time generated somewhat downstream of the leading edge. They found that the span-wise wave number at which the transient growth is maximum is much smaller than theoretically predicted. The investigations of Fransson *et al* [33], confirm the findings of White [31], and conclude that these discrepancies are due

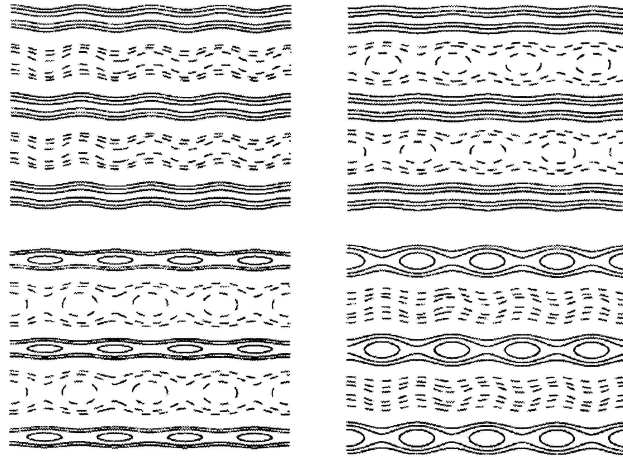


Figure 3. Contours of stream-wise velocity in the secondary instability of streaks. The solid and dashed lines represent low- and high-speed streaks respectively. Fundamental modes are shown on the left, and subharmonic ones on the right.

to span-wise vortices generated by roughness elements in the boundary layer. They show that experimentally generated streaks of very large amplitude are inviscidly stable to secondary instability. Incidentally, it was found in both computations and experiment that the presence of streaks has a stabilising effect on TS waves themselves. So it is clear that an alternate mechanism has to be in operation [23,25,26,34]. The studies of Corbett and Bottaro [35] on boundary layers in the presence of a stream-wise pressure gradient show again that the largest transient amplification results from stream-wise vortices.

In channels and pipes ‘bypass’ is the standard route to turbulence. In the former, linear instability occurs at extremely high Reynolds numbers, and the latter is linearly stable at all Reynolds numbers. In pipes, Faisst and Eckhardt [36] identified coherent structures moving with a constant wave speed, which cause breakdown to turbulence. The experiments of Hof *et al* [37] demonstrate the existence of finite amplitude disturbances arranged in specific patterns in the cross-section. A detailed discussion about these studies is beyond the scope of this paper, which is restricted to boundary layers.

3. The transition zone

The transition region (between x_t and fully developed turbulence) shown in figure 1 consists of localised turbulent patches (turbulent spots) surrounded by laminar flow. The spots are all arrowhead shaped. They grow self-similarly as they convect downstream and merge with one another (as seen in [20] and many later experiments). The head and rear move at fixed fractions of the flow velocity. An obvious quantitative description of the transition zone is in terms of the variation with x of the intermittency, γ (defined as the fraction of time for which the flow is turbulent).

With spots appearing randomly in accordance with a Poisson distribution in time and a uniform distribution in the span-wise coordinate z , γ would vary downstream as [38]

$$\gamma = 1 - \exp \left[\frac{-n\sigma}{U}(x - x_t)^2 \right]. \quad (9)$$

It is also useful to define an intermittency parameter [38], $F \equiv \sqrt{-\log(1 - \gamma)}$. If spot birth were to be totally random (as has been assumed hitherto) F would vary linearly in x . (We take it here that all the spots breakdown in the neighbourhood of x_t [38]. This is often a good assumption, and its validity is discussed in detail in [39].)

An important open question in this problem is that of how the birth of spots is related to the instability waves upstream. As far as we know, only empirical correlations between the two are in use. We have recently attempted [40] to provide a partial answer to this question. We consider the secondary instability of both TS waves and stream-wise streaks, and show that the moving two-dimensional pattern of maxima in disturbance vorticity can give rise to a spatio-temporal pattern in the birth of turbulent spots. The connection is especially clear in (i) the secondary instability of streaks and (ii) the oblique pattern arising out of TS waves in *adverse pressure gradient* boundary layers, such as would be formed in the flow past a wedge. This connection is established indirectly by comparing $F(x)$ obtained from a cellular automaton simulation to experiment. If spot birth is mostly regular in space and time, in a specific pattern with wavelengths and frequency as decreed by secondary instability, we find that the resulting $F(x)$ is nonlinear, with a slope that increases with x . The agreement with experimental measurements of intermittency in (i) and (ii) above is excellent, as seen in figure 4. Experiments in TS wave-driven transition on flat plate boundary layers, on the other hand, show a linear variation of F with x , in accordance with a random birth of spots. The reasons for this are discussed in [40]. This finding suggests that experiments performed in adverse pressure gradient (decelerating) boundary layers are likely to be ‘cleaner’, i.e., since there is less scope for randomness, spot birth is likely to be regular.

It is relevant to point out that in the experiments of Prigent *et al* [43] in plane Couette flow and Taylor–Couette flow, oblique patterns which precede turbulent spirals and spots have been observed. This sequence resembles what we expect is happening in boundary layers.

Complex interacting dynamical systems often display self-organised critical behaviour, i.e., they adjust themselves automatically to a state characterised by power-law correlations in both space and time [44]. This indicates that there is no characteristic length or time-scale that controls the behaviour of the system. In a transition zone dominated by a pattern of instability, we do not expect self-organised criticality. This is because (i) the frequency in the birth of spots and their downstream growth determine a length-scale of the transition zone and (ii) the pattern of highs and lows in the instability indicates some span-wise alignment in spot birth, which should lead to modulations of known wavelength in the downstream behaviour. The probability density function of the persistence time w_t of laminar flow, defined as the extent of time that the flow continuously remains laminar is plotted in figure 5. The expectations above are borne out. In the case of random

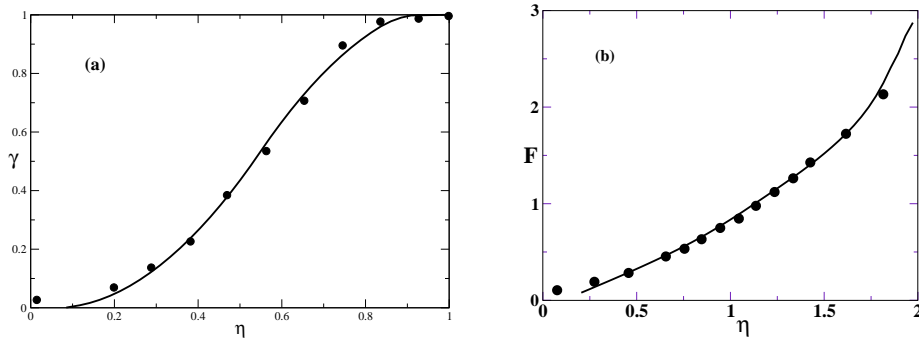


Figure 4. Variation of the intermittency with x . Line: stochastic simulation [40], spot birth according to the dominant instability mode; symbols: experiment, (a) in an adverse pressure gradient flow [41] (b) streak breakdown on a flat plate boundary layer [42].

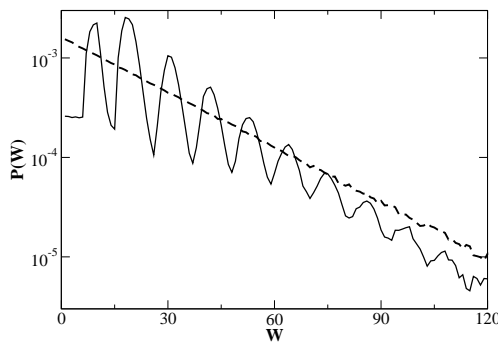


Figure 5. Probability density function (PDF) of 'waiting time' [40].

breakdown, the probability distribution function (PDF) of the persistence time decays exponentially with persistence time, whereas in the case of regular breakdown, there is significant modulation.

4. Conclusions

There are many issues not examined in this paper, such as the effect of wall roughness, about which a lot of recent research has focussed. We have restricted our review to some of what is known about the later stages of transition to turbulence in a boundary layer. Background disturbances play a large role in determining how and when transition will take place. Our recent work shows that spot birth is likely to be determined (at least in part) by the pattern of instability preceding this stage.

Acknowledgements

The authors thank the Defence Research and Development Organisation, Government of India, for providing financial support for this work.

References

- [1] C C Lin, *The theory of hydrodynamic stability* (Cambridge University Press, London, 1955)
- [2] S Chandrasekhar, *Hydrodynamics and hydromagnetic stability* (Oxford University Press, London, 1961)
- [3] P G Drazin and W H Reid, *Hydrodynamic stability* (Cambridge University Press, London, 1981)
- [4] P Huerre and M Rossi, Hydrodynamic instabilities in open flows, in *Hydrodynamics and nonlinear instabilities* edited by C Godreche and P Manneville (Cambridge University Press, Cambridge, 1998) pp. 81–288
- [5] P J Schmid and D S Henningson, *Stability and transition in shear flows* (Springer, New York, 2001)
- [6] W M F Orr, *Proc. R. Irish Acad.* **27(3)**, 69 (1907)
- [7] A Sommerfeld, *Proc. Fourth Int. Cong. Math.*, Rome, **III**, 116 (1906)
- [8] W Tollmien, *Nacher. ges. Wiss. Gottingen, Math-phys. Kl.* (1929) pp. 21–24
- [9] Schlichting, Zur entstehung der turbulenz bei der plattenstromung, *Nachr. Ges. Wiss. Gottingen, Math-phys. Kl.* (1933) pp. 181–208
- [10] G B Schubauer and H Skramstad, *J. Res. Nat. Bur. Standards* **38**, 251 (1947)
- [11] H B Squire, *Proc. R. Soc. London A*, **142**, 621 (1933)
- [12] T Herbert, *Annu. Rev. Fluid Mech.* **20**, 487 (1988)
- [13] K H Bech, D S Henningson and R A W M Henkes, *Phys. Fluids* **10(6)**, 1405 (1998)
- [14] H L Reed and W S Saric, *Ann. Rev. Fluid Mech.* **28**, 389 (1996)
- [15] W S Saric, H L Reed and E B White, *Ann. Rev. Fluid Mech.* **35**, 413 (2003)
- [16] P S Klebanoff, K D Tidstorm and L M Sargent, *J. Fluid. Mech.* **12**, 1 (1962)
- [17] A R Wazzan, *Prog. Aerosp. Sci.* **16(2)**, 99 (1975)
- [18] Y S Kachanov, V Kozlov and V Y Levchenko, *Izv. Akad. Nauk SSSR, Mekh. Zhidk. Gaza* **3**, 49 (1977)
- [19] R Govindarajan, V S L’vov, I Procaccia and A Sameen, *Phys. Rev.* **E67**, 026310 (2003)
- [20] H Emmons, *J. Aero. Sci.* **18**, 490 (1951)
- [21] T Ellingsen and E Palm, *Phys. Fluids* **18**, 487 (1975)
- [22] L Trefethen, A Trefethen, S Reddy and T Driscoll, *Science* **261**, 578 (1993)
- [23] P Andersson, L Brandt, A Bottaro and D Henningson, *J. Fluid Mech.* **428**, 29 (2001)
- [24] L Brandt and D Henningson, *J. Fluid Mech.* **472**, 229 (2002)
- [25] L Brandt, C Cossu, J M Chomaz, P Huerre and D Henningson, *J. Fluid Mech.* **485**, 221 (2003)
- [26] A V Boiko, K J A Westin, B G B Klingmann, V V Kozlov and P H Alfredson, *J. Fluid Mech.* **281**, 219 (1994)
- [27] P Andersson, M Berggren and D S Henningson, *Phys. Fluids* **11**, 134 (1999)
- [28] M T Landahl, *SIAM J. Appl. Math.* **28**, 735 (1975)
- [29] M T Landahl, *J. Fluid Mech.* **98**, 243 (1980)
- [30] A V Boiko, *Eur. J. Mech. B Fluids* **21**, 325 (2002)

- [31] E B White, *Phys. Fluids* **14**, 4429 (2002)
- [32] A V Boiko and H H Chun, *Phys. Fluids* **16**, 3153 (2004)
- [33] J H M Fransson, L Brandt, A Talamelli and C Cossu, *Phys. Fluids* **16**, 3627 (2004)
- [34] C Cossu and L Brandt, *Phys. Fluids* **14**, L57 (2002)
- [35] P Corbet and A Bottaro, *Phys. Fluids* **12**, 120 (2000)
- [36] H Faisst and B Eckhardt, *Phys. Rev. Lett.* **91**(22), 4502 (2003)
- [37] B Hof, C W H van Doorne, J Westerweel, F T M Nieuwstadt, H Faisst, B Eckhardt, H Wedin, R R Kerswell and F Waleffe, *Science* **305**, 1594 (2004)
- [38] R Narasimha, *J. Aero. Sci.* **24**, 711 (1957)
- [39] N Vinod and R Govindarajan, *Phys. Rev. E* (in preparation)
- [40] N Vinod and R Govindarajan, *Phys. Rev. Lett.* **93**, 114501 (2004)
- [41] J Gostelow and A Blunden, *33rd ASME International Gas Turbine and Aeroengine Congress* (Amsterdam, Netherlands, 1988)
- [42] M Matsubara and P H Alfredsson, *J. Fluid. Mech.* **430**, 149 (2001)
- [43] A Prigent, G Grégoire, H Chaté, O Dauchot and W van Saarloos, *Phys. Rev. Lett.* **89**(1), 014501 (2002)
- [44] P Bak, C Tang and K Wiesenfeld, *Phys. Rev. Lett.* **59**, 381 (1987)